

# Does a Nambu-Goto wall emit gravitational waves?

– Cylindrical Nambu-Goto wall as an example of gravitating non-spherical walls –

Kouji Nakamura\*

*Division of Theoretical Astrophysics, National Astronomical Observatory,  
Mitaka, Tokyo 181-8588, Japan*

(January 2, 2019)

Gravitational field of a cylindrical Nambu-Goto wall in the vacuum spacetime is considered in order to clarify the interaction between Nambu-Goto membranes and gravitational waves. If one neglects the emission of gravitational waves by the wall motion, the spacetime becomes singular. It is also shown that the emission of gravitational waves does occur by the motion of the cylindrical wall if the initial data is singularity free. The energy loss rate due to radiation of gravitational waves agrees with that estimated from the test wall motion and the quadrupole formula for the gravitational wave emission. This is quite different from the oscillatory behavior of gravitating Nambu-Goto membranes: the presence of gravity induces the wall to lose its dynamical degree of freedom.

PACS numbers: 04.40.-b, 11.27.+d

## I. INTRODUCTION

Gravitational field and dynamics of extended objects (membranes) are familiar topics in recent physics. Historically, gravity of membranes is investigated in the context of topological defects formed during phase transition in the early universe [1,2]. Among these extended objects, domain walls are the simplest type of defects which arose when the phase transition has occurred by the breakdown of a discrete symmetry. However, the theoretical prediction using standard scaling defect models are in conflict with observations of the Cosmic Background Explorer satellite [3]. Further, stable domain wall networks are not allowed in the early universe because they overdominate the radiation energy density [1,2]. Despite of these discouraging results, topological defects have been remained intrinsically interesting topics to study extended objects. Unstable defects formed in the early universe might radiate gravitational waves by their rapid oscillation [4] and then the detection of relic gravitational waves from these extended objects is considered to be one of the evidences for the phase transition in the universe. Moreover, as seen in the recent proposal of the theoretical models with the large extradiimension [6], so called brane world scenario, domain walls are considered as a realization of our universe in higher dimensions.

Within the general relativity, topological defects are unusual and are expected to play a role of an interesting source of gravity. In the simplest case, domain walls are idealized by the infinitesimally thin Nambu-Goto membranes. If the self-gravity of membranes is ignored (test membrane case), the Nambu-Goto action admits oscilla-

tory solutions which radiate gravitational waves as mentioned above. However, by taking into account the self-gravity of the Nambu-Goto wall, it is shown that self-gravitating walls coupled to gravitational wave behave in a quite different manner. The dynamical degrees of freedom concerning the perturbative oscillations around spherical walls is given by that of gravitational waves, and self-gravitating spherical walls do not oscillate spontaneously contrary to the case of test walls [7]. The essentially same conclusion is also obtained in the case of an infinite Nambu-Goto string [8]. These results insist that the motion of gravitating membranes is quite different from the motion of the test membranes even if the total energy of the wall is very small. This difference between test membranes and self-gravitating membranes is crucial when one estimates the energy of the gravitational waves from these extended objects.

In this paper, we investigate the gravitational wave emission due to the motion of a Nambu-Goto wall. Particularly, we consider the cylindrically symmetric domain wall as a toy model of highly elongated gravitating walls. The results that the gravitating Nambu-Goto membrane has no dynamical degree of freedom of are based on the perturbation around the spacetime without gravitational wave. We expect that the behavior of highly distorted Nambu-Goto walls is different. The cylindrically symmetric spacetime considered here is described by the metric of the *Weyl canonical form*. In this metric, there are cylindrically symmetric wave modes, which is called *Einstein-Rosen wave* (ER wave), and a domain wall's motion excites ER wave. We have to treat the coupled system of ER wave and the cylindrically symmetric domain wall, which is governed by the Einstein equation and the

---

\*E-mail:kouchan@th.nao.ac.jp

junction condition [9] on the wall.

We first show that all spacetimes containing a cylindrical wall become singular if we neglect ER wave emission. This implies that, in the absence of singularities, ER wave emission necessarily occurs by the motion of the cylindrical wall. Next, we consider the momentarily static “regular” initial data for the spacetime containing a cylindrical domain wall and their infinitesimal time evolution. We show that the monotonically collapsing motion of the gravitating cylindrical wall does emit gravitational waves and that the estimate of the energy of gravitational waves using the quadrupole formula is correct if the wall energy density is sufficiently small. This is the quite reasonable result expected from the behavior of the Nambu-Goto membrane in the absence of gravity. However, we have to notice that this result has an apparent discrepancy with the results in Ref. [7,8].

The organization of this paper is as follows. In the next section, we briefly review the symmetry reduction of spacetime into the cylindrically symmetric one. We also derive the basic equations that govern the motion of the domain wall. In Sec.III, we consider the possible solutions of a self-gravitating domain wall without gravitational wave emission. In Sec.IV, we set up momentarily static and radiation free regular initial configurations and investigate the time evolution to see the gravitational wave emission due to the wall motion. Finally, Sec.V is devoted to the summary and discussions about the discrepancy with the conclusion in Ref. [7,8].

Throughout this paper, we use the unit such that the light velocity  $c = 1$  and Newton’s gravitational constant is denoted by  $G$ . The signature of Lorentzian metrics is chosen to be  $(-, +, +, +)$ .

## II. CYLINDRICAL SPACETIME WITH A DOMAIN WALL

We consider the spacetime with a cylindrical domain wall using the thin wall approximation. The whole spacetime  $(\mathcal{M}, g_{ab})$  contains two vacuum regions  $(\mathcal{M}_+, g_{ab+})$  and  $(\mathcal{M}_-, g_{ab-})$ . Each region  $(\mathcal{M}_+$  or  $\mathcal{M}_-$ ) has a time-like boundary  $\Sigma_\pm$ , respectively, which should be identified so that  $\Sigma := \Sigma_+ = \Sigma_-$  using Israel’s junction condition [9]. The whole spacetime is  $\mathcal{M} = \mathcal{M}_- \cup \Sigma \cup \mathcal{M}_+$ . The timelike submanifold  $\Sigma$  is the world volume of the domain wall.

Since we consider the domain wall with cylindrical symmetry, it is natural to consider the vacuum region  $\mathcal{M}_\pm$  also have cylindrical symmetry. The cylindrically symmetric spacetime considered in this paper has two commutable spacelike Killing vector fields  $z^\alpha$  and  $\phi^\alpha$  and these are both hypersurface orthogonal. The orbit of  $z^\alpha$  is  $R^1$  and that of  $\phi^\alpha$  is  $S^1$ . We introduce coordinate functions  $z$  and  $\phi$  by  $z^\alpha \nabla_\alpha z = 1$  and  $\phi^\alpha \nabla_\alpha \phi = 1$ , respectively.  $\phi$  is a periodic coordinate with the period  $2\pi$ .

Using one of the vacuum Einstein equations  $R_z^z + R_\phi^\phi =$

0 and assuming that the gradient of  $\sqrt{(\phi^\alpha \phi_\alpha)(z^\alpha z_\alpha)}$  is spacelike, the both metrics on the spacetime  $\mathcal{M}_\pm$  are reduced to the *Weyl canonical form*:

$$ds^2 = e^{2(\gamma-\psi)}(-dt^2 + dr^2) + e^{2\psi} dz^2 + r^2 e^{-2\psi} d\phi^2, \quad (2.1)$$

where  $\psi$  and  $\gamma$  depend on  $t$  and  $r$ . The existence of a thin wall does not contradict to the assumption that the gradient of  $\sqrt{(\phi^\alpha \phi_\alpha)(z^\alpha z_\alpha)}$  is spacelike. (See Appendix A.) The coordinates  $t$  and  $r$  parameterize the two-dimensional orbit space  $\mathcal{N}$  and each point on  $\mathcal{N}$  corresponds to a cylinder of symmetry. Further, we call the direction to which  $t$  increases (decreases) “future” (“past”) direction.

The vacuum Einstein equations for the metric (2.1) are given by

$$\partial_t^2 \psi - \frac{1}{r} \partial_r (r \partial_r \psi) = 0, \quad (2.2)$$

$$\partial_r \gamma = r ((\partial_t \psi)^2 + (\partial_r \psi)^2), \quad (2.3)$$

$$\partial_t \gamma = 2r (\partial_t \psi) (\partial_r \psi). \quad (2.4)$$

Eq.(2.2) is the wave equation and  $\psi$  corresponds to the plus mode of gravitational waves, so called *Einstein-Rosen wave* (ER wave).

The timelike curve  $\Sigma \cap \mathcal{N}$  is the trajectory of the domain wall in  $\mathcal{N}$ . The future directed unit tangent  $u^\alpha$  ( $u^\alpha u_\alpha = -1$ ) of this timelike curve is the 4-velocity of the domain wall and the proper time  $\tau$  of the domain wall is introduced by  $u^\alpha \nabla_\alpha \tau = 1$ . Since we consider the cylindrically symmetric domain wall with the Killing vectors  $z^\alpha := z_\pm^\alpha$  and  $\phi^\alpha := \phi_\pm^\alpha$  on  $\Sigma_\pm$ , the coordinate functions  $z$  and  $\phi$  on  $\mathcal{M}_\pm$  are extended to smooth functions on the whole spacetime  $\mathcal{M}$ . Then the coordinate system  $(\tau, z, \phi)$  on  $\Sigma$  is naturally induced.

The induced metrics on  $\Sigma_\pm$  from  $g_{ab\pm}$  are given by

$$h_{ab\pm} = -(d\tau)_a (d\tau)_b + e^{2\Psi_\pm(\tau)} (dz)_a (dz)_b + R_\pm^2(\tau) e^{-2\Psi_\pm(\tau)} (d\phi)_a (d\phi)_b, \quad (2.5)$$

where  $\Psi_\pm(\tau) = \psi|_{\Sigma_\pm}$  and  $R_\pm(\tau) = r|_{\Sigma_\pm}$ , respectively. Since  $\Sigma_\pm$  should be diffeomorphic to each other to identify them,  $h_{ab\pm}$  must satisfy  $h_{ab} := h_{ab+} = h_{ab-}$  in the above coordinate system:

$$R(\tau) := R_+ = R_-, \quad \Psi(\tau) := \Psi_+ = \Psi_-. \quad (2.6)$$

Further, the identification should be done so that  $n_{a+} = n_{a-}$ , where  $n_{a\pm}$  are unit normal to  $\Sigma_\pm$  directed from  $\mathcal{M}_-$  to  $\mathcal{M}_+$ . The existence of the domain wall gives the finite discontinuity of the extrinsic curvature  $K_{b\pm}^a$  of  $\Sigma_\pm$  in  $\mathcal{M}_\pm$ , where  $K_{b\pm}^a := h^{ac} h_b^d \nabla_c^\pm n_{d\pm}$ , and  $\nabla_a^\pm$  is the covariant derivatives associated with the metric  $g_{ab\pm}$ , respectively. When the surface energy on  $\Sigma$  is given by  $S_b^a = \sigma h_b^a$ , the Israel’s junction conditions becomes to  $[K_b^a] = -\lambda h_b^a$  [10].  $\lambda = 4\pi G \sigma > 0$  is the surface tension of the wall which is equal to the surface density.

In terms of the coordinate system in Eq.(2.1),  $u^\alpha$  is given by

$$u^a = u_{\pm}^t \left( \frac{\partial}{\partial t} \right)_{\pm}^a + u^r \left( \frac{\partial}{\partial r} \right)_{\pm}^a, \quad (2.7)$$

$$u^r = \frac{dR}{d\tau}, \quad u_{\pm}^t = \frac{dT_{\pm}}{d\tau} = \sqrt{\left( \frac{dR}{d\tau} \right)^2 + e^{-2(\Gamma_{\pm} - \Psi_s)}}, \quad (2.8)$$

where  $\Gamma_{\pm} := \gamma(t, r)|_{\Sigma_{\pm}}$  and  $T_{\pm} := t|_{\Sigma_{\pm}}$ .  $u_{\pm}^t$  are positive because  $u^a$  is future directed. From the orthonormal condition  $n_{\pm}^a n_{a\pm} = 1$  and  $u^a n_{a\pm} = 0$ ,  $n_{\pm}^a$  are given by

$$n_{\pm}^a = \epsilon_{\pm} \left( u^r \left( \frac{\partial}{\partial t_{\pm}} \right)_{\pm}^a + u_{\pm}^t \left( \frac{\partial}{\partial r} \right)_{\pm}^a \right), \quad (2.9)$$

where  $\epsilon_{\pm} = \text{sgn}(n_{\pm}^a \partial_a r)$ . Using Eqs.(2.7)-(2.9), the all components of the junction condition for the extrinsic curvature of  $\Sigma$  are given by

$$\left( \frac{d^2 R}{d\tau^2} - \frac{dR}{d\tau} D_{\parallel} \psi + R (D_{\parallel} \psi)^2 \right) \left[ \frac{1}{D_{\perp} r} \right] + R \left[ \frac{(D_{\perp} \psi)^2}{D_{\perp} r} \right] = -2\lambda, \quad (2.10)$$

$$[D_{\perp} \psi] = -\lambda, \quad (2.11)$$

$$[D_{\perp} r] = -2\lambda R. \quad (2.12)$$

where  $D_{\parallel} A = u^a \nabla_a A$ ,  $(D_{\perp} A)_{\pm} = (n^a \nabla_a A)_{\pm}$  for an arbitrary function  $A$  in the neighborhood of  $\Sigma$  and the subscript  $\pm$  shows the functions evaluated on  $\Sigma_{\pm}$ , respectively. Further, we note  $[D_{\parallel} \psi] = 0 = [D_{\parallel} r]$ .

Eq.(2.10) is the equation of motion for the cylindrical wall  $\Sigma$  and Eq.(2.11) is the boundary condition for ER wave  $\psi$  on  $\Sigma$ . Eq.(2.12) is also rewritten by

$$\left( \frac{dR}{d\tau} \right)^2 - (\lambda R)^2 - \frac{1}{4\lambda R} (e^{-2\Gamma_+} - e^{-2\Gamma_-})^2 + \frac{1}{2} (e^{-2\Gamma_+} + e^{-2\Gamma_-}) e^{\Psi} = 0 \quad (2.13)$$

by virtue of Eq.(2.9). We note that Eq.(2.10) is derived from Eqs.(2.11) and (2.12) by using Eqs.(2.2)-(2.4) and Eq.(2.8).

We explicitly see that the behavior of the ER wave at the boundary ( $\Psi$  and  $\Gamma_{\pm}$ ) affects the wall motion by Eq.(2.13) and the wall motion affects  $\psi$  and  $\gamma$  by their boundary conditions Eq.(2.11). Thus, this is the radiation reaction problem. To clarify the dynamics of a gravitating cylindrical domain wall, we have to solve the equations Eqs.(2.2)-(2.4) with the boundary conditions Eq.(2.11) and Eq.(2.12) on  $\Sigma$  simultaneously, in general. In this paper, we show that the cylindrical domain wall must emit gravitational waves using these equations and boundary conditions.

### III. SELF-GRAVITATING DOMAIN WALL WITHOUT GRAVITATIONAL WAVE EMISSION

In this section, we consider the self-gravitating domain wall spacetime without gravitational wave emission and

show that all solutions contain singular axes.

Since  $\mathcal{M}_{\pm}$  considered here is static, we assume that

$$\partial_t^2 \psi = \partial_t \psi = 0. \quad (3.1)$$

The static solution to Eqs.(2.2)-(2.4) is

$$\psi = -\kappa \ln \left( \frac{r}{R_0} \right), \quad \gamma = \gamma_0 + \kappa^2 \ln \left( \frac{r}{R_0} \right). \quad (3.2)$$

where  $R_0$ ,  $\gamma_0$  and  $\kappa$  are constants and the line element is given by

$$ds^2 = e^{2\gamma_0} \left( \frac{r}{R_0} \right)^{2(\kappa^2 + \kappa)} (-dt^2 + dr^2) + \left( \frac{r}{R_0} \right)^{-2\kappa} dz^2 + r^2 \left( \frac{r}{R_0} \right)^{2\kappa} d\phi^2. \quad (3.3)$$

This is well-known as the Levi-Civita metric [11].

The circumferential radius of the symmetric cylinder  $dt = dr = 0$ ,

$$\tilde{r}(r) := \frac{1}{2\pi} \int_0^{2\pi} d\phi \sqrt{g_{\phi\phi}}, \quad (3.4)$$

tells us the axis of the cylindrical symmetry. When  $\kappa + 1 > 0$ ,  $\tilde{r}(r)$  is a monotonically increasing function of  $r$  and vanishes at  $r = 0$ . This means that  $r = 0$  is the axis of symmetry in this case. On the other hand,  $\tilde{r}(r)$  monotonically decreases and vanishes at  $r = \infty$  when  $\kappa + 1 < 0$ . Then,  $r = \infty$  is the axis of cylindrical symmetry in the case of  $\kappa + 1 < 0$ .

The square of the Riemann curvature for the metric (3.3) is given by

$$I := R_{abcd} R^{abcd} = \frac{16\kappa^2(1+\kappa)^2(1+\kappa+\kappa^2)}{R_0^4 e^{4\gamma_0}} \left( \frac{R_0}{r} \right)^{4(\kappa^2 + \kappa + 1)}. \quad (3.5)$$

We note that the curvature of the spacetime approaches to zero as  $I \propto r^{-3-(2\kappa+1)^2} \rightarrow 0$  only when  $r \rightarrow \infty$ . On the other hand, when  $r \rightarrow 0$ ,  $I$  diverges, except the cases  $\kappa = 0$  or  $-1$ . When  $\kappa = 0$  or  $-1$ , the metric (3.3) is locally flat.

Here, we consider the construction of the whole spacetime  $\mathcal{M} = \mathcal{M}_+ \cup \Sigma \cup \mathcal{M}_-$  with the metrics (3.3) on  $\mathcal{M}_{\pm}$ . We denote  $\gamma_0$  and  $\kappa$  on each  $\mathcal{M}_{\pm}$  by  $\gamma_{0\pm}$  and  $\kappa_{\pm}$ , respectively. The junction conditions Eqs.(2.6) are given by

$$\ln \left( \frac{R}{R_0} \right)^{\kappa_+} = \ln \left( \frac{R}{R_0} \right)^{\kappa_-}, \quad (3.6)$$

and the conditions (2.11) and (2.12) become to

$$\epsilon_+ \kappa_+ u_+^t - \epsilon_- \kappa_- u_-^t = \lambda R \quad (3.7)$$

$$\epsilon_+ u_+^t - \epsilon_- u_-^t = -2\lambda R. \quad (3.8)$$

To evaluate Eqs.(3.6)-(3.8), and (2.10), we consider two cases,  $\kappa_+ \neq \kappa_-$  and  $\kappa_+ = \kappa_-$ , separately.

### A. $\kappa_+ \neq \kappa_-$ case

In this case, Eq.(3.6) must hold for arbitrary  $\tau$ , i.e.,

$$R(\tau) = R_0, \quad \frac{dR}{d\tau} = 0. \quad (3.9)$$

These mean the domain wall should stay at  $r = R_0$ . Then the components of the 4-velocity (2.8) are given by

$$u^r = 0, \quad u_{\pm}^t = e^{-\gamma_{0\pm}}. \quad (3.10)$$

The conditions (3.7) and (3.8) are given by

$$\epsilon_{\pm} u_{\pm}^t = \frac{1 + 2\kappa_{\mp}}{\kappa_+ - \kappa_-} \lambda R_0, \quad (3.11)$$

which shows that  $\epsilon_{\pm}$  are determined by

$$\epsilon_{\pm} = \text{sgn} \left( \frac{1 + 2\kappa_{\mp}}{\kappa_+ - \kappa_-} \right). \quad (3.12)$$

Eq.(2.10) gives the acceleration of the wall:

$$\frac{d^2 R}{d\tau^2} = - \frac{(1 + 2\kappa_+)(1 + 2\kappa_-)}{2(\kappa_+ - \kappa_-)^2} \times (\kappa_+ + \kappa_- + 2\kappa_+ \kappa_- + 2) \lambda^2 R_0. \quad (3.13)$$

Since Eqs.(3.9) should hold for arbitrary  $\tau$ , ( $d^2 R/d\tau^2$ ) = 0 for arbitrary  $\tau$ . We easily see that  $\kappa_{\pm} \neq 1/2$  from Eqs.(3.11) and  $\kappa_- \neq \kappa_+$ . Then  $\kappa_{\pm}$  should satisfy the relation

$$\kappa_+ + \kappa_- + 2\kappa_+ \kappa_- + 2 = 0. \quad (3.14)$$

This is the condition obtained by Tomita [12].

From the relation (3.14) and Eq.(3.12), we obtain  $(\epsilon_-, \epsilon_+) = (+, -)$ , which means that the coordinate function  $r$  is maximum at  $\Sigma$  and both  $\mathcal{M}_{\pm}$  include the axis  $r = 0$ . Eq.(3.14) also forbids the cases that both of  $\kappa_{\pm}$  are 0 or  $-1$ . Then, one of the axis  $r = 0$  has to be singular.

### B. $\kappa_+ = \kappa_-$ case

In this case, we obtain  $\kappa_{\pm} = -1/2$  from Eqs.(3.7) and (3.8). The condition Eq.(3.6) is trivially satisfied. Then, the domain wall may move on  $\mathcal{N}$ . The equation (2.13) of the wall motion is given by

$$\left( \frac{dR}{d\tau} \right)^2 + V(R) = 0, \quad (3.15)$$

$$V(R) = -(\lambda R)^2 - \frac{1}{(4\lambda)^2 R R_0} (e^{-2\gamma_{0+}} - e^{-2\gamma_{0-}}) + \frac{1}{2} (e^{-2\gamma_{0-}} + e^{-2\gamma_{0+}}) \left( \frac{R}{R_0} \right)^{1/2}. \quad (3.16)$$

Actually, Eq.(3.15) has the solutions of a moving domain wall without gravitational waves [13]. From the energy condition,  $\lambda > 0$ , and the condition (3.8), the case  $(\epsilon_-, \epsilon_+) = (-, +)$  is rejected. Then,  $\mathcal{M}$  must have the axis  $r = 0$  in itself. Since  $\kappa_{\pm} = -1/2$  (neither 0 nor  $-1$ ), the axis is singular.

## IV. EINSTEIN-ROSEN WAVE EMISSION FROM CYLINDRICAL DOMAIN WALL

In the previous section, we have seen the all spacetimes with a self-gravitating cylindrical domain wall without gravitational waves have to include singular axes in itself. This implies that we should take into account the emission of gravitational waves if we require the regularity of the spacetime and the emission of gravitational waves necessarily occurs. To see this, we consider the infinitesimal time evolution from a “regular” initial configuration. In this paper, we regard that the initial surface is *regular* if the initial surface does not include scalar polynomial singularities or deficit angles except the delta-function matter distribution of the wall. We concentrate on the momentarily static and radiation free initial configuration, and its infinitesimal time evolution, for simplicity. Then, we see that ER wave emission does occur due to the motion of the wall.

The total system of a self-gravitating domain wall in the cylindrically symmetric spacetime is governed by the Einstein equations (2.2)-(2.4), the junction conditions for the intrinsic metric (2.6), and those for the extrinsic curvature (2.10)-(2.12). Among them, Eqs.(2.2) and (2.10) are evolution equations and Eqs.(2.3), (2.4), (2.6), (2.11) and (2.12) are constraint equations which the initial data should be satisfied. By the small modification of the static wall solutions in the previous section, we obtain the momentarily static initial configurations that satisfy these constraints.

### A. Momentarily static initial configurations

Let  $\mathcal{S}$  be a momentarily static initial space and  $\mathcal{P} = \mathcal{S} \cap \Sigma$  is the initial locus of the wall on  $\mathcal{S}$ . Then  $\mathcal{P}$  divides  $\mathcal{S}$  into two parts:  $\mathcal{S}_{\pm} := \mathcal{S} \cap \mathcal{M}_{\pm}$ . We choose the origin of the comoving time  $\tau = 0$  at  $\mathcal{P}$ .

Further, we consider the radiation free initial condition, where there is neither incidental nor outgoing ER waves on  $\mathcal{S}$ , i.e.,  $\partial_t^2 \psi_{\mathcal{S}_{\pm}}(r) = \partial_t \psi_{\mathcal{S}_{\pm}}(r) = 0$ . Then  $\psi_{\mathcal{S}_{\pm}}(r)$  and  $\gamma_{\mathcal{S}_{\pm}}(r)$  are given by the same form as Eq.(3.2). In Eq.(3.2), we denote  $\gamma_0$  and  $\kappa$  on  $\mathcal{S}_{\pm}$  by  $\gamma_{0\pm}$  and  $\kappa_{\pm}$  as in the last section. We consider the situation where the wall is  $r = R_0$  initially as Eqs.(3.9). By this choice, Eqs.(2.6) are trivially satisfied.

Next, we evaluate the junction conditions (2.10)-(2.12). First, from (2.11) and (2.12), we easily see that  $\kappa_+ \neq \kappa_-$  by the regularity on  $\mathcal{S}$ . Actually, if  $\kappa_+ = \kappa_-$ , (2.11) and (2.12), which have the same form as Eqs.(3.7)

and (3.8), shows that the axis  $r = 0$  is singular as seen in the last section. Further, the condition of Eqs.(3.8) together with the energy condition  $\lambda > 0$  and the  $u_{\pm}^t > 0$  leads  $(\epsilon_-, \epsilon_+) = (+, \pm)$  [14] and  $\mathcal{S}_-$  includes the axis  $r = 0$ . Then  $\kappa_+ \neq \kappa_-$ . This means Eqs.(3.10)-(3.12) are also true on  $\mathcal{S}$ .

In contrast to the results in Sec.III A, the relation (3.14), which was obtained from Eq.(2.10), does not hold, since it contradicts to the regularity of  $\mathcal{S}$  as seen in the last section. Instead, the initial acceleration of the domain wall Eq.(3.13) does not vanish. Then the domain wall begins to move and the system evolves to the dynamical phase. The regular initial configurations are classified into two cases:  $(\epsilon_-, \epsilon_+) = (+, +), (+, -)$ . In these cases, the motion of the wall is different. Then, we consider these cases, separately.

### 1. $\epsilon_+ = 1$ case

To avoid the curvature singularity at  $r = 0$  in  $\mathcal{S}_-$ ,  $\kappa_-$  should be  $-1$  or  $0$ . In the following, we may concentrate only on the case  $\kappa_- = 0$  because  $\kappa_- = -1$  case is locally equivalent to the case  $\kappa_- = 0$ . Actually, when  $\kappa_- = -1$ ,  $z$  should be a periodic coordinate with the period  $2\pi R_0 e^{\gamma_{0-}}$  to avoid the conical singularity at  $r = 0$  and the Killing orbit of  $z^a$  on  $\mathcal{S}_-$  is not  $R^1$  but  $S^1$ . Since  $z$  is extended as a function on the whole spacetime  $\mathcal{M}$ ,  $z$  is also a periodic coordinate on  $\mathcal{S}_+$ . We can easily check that this case is equivalent to the case  $\kappa_- = 0$  with the above periodicity of  $z$  by the following replacements:  $e^{\gamma_{0-}t} \rightarrow t$ ,  $e^{\gamma_{0-}r} \rightarrow r$ ,  $e^{-\gamma_{0-}z/R_0} \rightarrow \phi$ ,  $R_0\phi \rightarrow z$ ,  $-\kappa_+ - 1 \rightarrow \kappa_+$ ,  $e^{\gamma_{0-}R_0} \rightarrow R_0$  and  $\gamma_{0+} - \gamma_{0-} \rightarrow \gamma_{0+}$ .

When  $\kappa_- = 0$ , the conical singularity avoidance at  $r = 0$  in  $\mathcal{S}_-$  leads  $\gamma_{0-} = 0$ . Then, Eqs.(3.11) give

$$u_+^t = 1 - 2\lambda R_0, \quad u_-^t = 1, \quad (4.1)$$

$$\kappa_+ = \frac{\lambda R_0}{1 - 2\lambda R_0}, \quad e^{-\gamma_{0+}} = 1 - 2\lambda R_0. \quad (4.2)$$

Since  $u^a$  is future directed ( $u_+^t > 0$ ), Eqs.(4.1) lead

$$0 < R_0 < \frac{1}{2\lambda}, \quad (4.3)$$

and  $\kappa_+$  must be positive. The initial acceleration of the wall is

$$\left(\frac{d^2 R}{d\tau^2}\right)_0 = -\frac{2 - 3\lambda R_0}{2R_0}. \quad (4.4)$$

By virtue of (4.3), Eq.(4.4) is the negative acceleration, i.e., the wall begins to collapse.

The geometry of the initial surface  $\mathcal{S}$  is seen by evaluating the relation between circumferential radius  $\tilde{r}$  of the symmetric cylinder defined by Eq.(3.4) and the proper radial distance  $\rho$  defined by

$$d\rho = e^{\gamma - \psi} dr = e^{\gamma_{0+}} \left(\frac{r}{R_0}\right)^{\kappa_+ + \kappa_+} dr, \quad (4.5)$$

which is easily obtained by

$$\frac{d\tilde{r}}{d\rho} = \frac{1 + \kappa_+}{e^{\gamma_{0+}}} \left\{ \frac{(\kappa_+^2 + \kappa_+ + 1)\rho}{e^{\gamma_{0+}R_0}} \right\}^{\frac{-\kappa_+^2}{\kappa_+^2 + \kappa_+ + 1}}. \quad (4.6)$$

Since  $\kappa_+ > 0$ ,  $\tilde{r}(r)$  of the symmetric cylinder in  $\mathcal{S}_+$  is a monotonically increasing function of  $r$ . Then,  $\mathcal{S}_+$  has infinity in the radial direction. Further, in the limit  $\lambda R_0 \rightarrow 0$ , (“mass per unit proper  $z$  length”  $\rightarrow 0$ ), we see  $\kappa_+ \rightarrow 0$  and  $\gamma_{0+} \rightarrow 0$ . It means  $\mathcal{S}_+$  approaches to the flat space, i.e.,  $d\tilde{r}/d\rho \rightarrow 1$ . We call this limit as “*the weak gravity limit*”. This is the counter part of the test wall case. In the limit  $\lambda R_0 \rightarrow 1/2$ , (equivalently “mass per unit proper  $z$  length”  $\rightarrow 1/(4G)$ ), the initial configuration characterized by Eqs.(4.2) looks singular. In this limit,  $d\tilde{r}/d\rho \rightarrow 0$ , which means the circumference is constant outward. This curious geometry of  $\mathcal{S}_+$  comes from the strong gravitational effect of the wall. We call this limit as “*the strong gravity limit*”. (See Appendix A.)

### 2. $\epsilon_+ = -1$ case

In this case, both  $\mathcal{S}_{\pm}$  contain the points  $r = 0$  and we impose the regularity there. To avoid the curvature singularity,  $\kappa_-$  should be  $0$  or  $-1$ . When  $\kappa_- = 0$ , we choose  $\gamma_{0-} = 0$  to avoid the conical singularity at  $r = 0$  on  $\mathcal{S}_-$ . Then  $\mathcal{S}_-$  is flat.  $\kappa_+ \neq \kappa_- = 0$  and the regularity at  $r = 0$  in  $\mathcal{S}_+$  yields  $\kappa_+ = -1$ . Eqs.(3.11) and (3.10) tell us  $\lambda R_0 = 1$  and  $\gamma_{0+} = 0$ . Then  $\mathcal{S}_+$  is also flat and the metric on  $\mathcal{S}_+$  is given by

$$ds^2 = -dt^2 + dr^2 + \left(\frac{r}{R_0}\right)^2 dz^2 + R_0^2 d\phi^2. \quad (4.7)$$

From the regularity at  $r = 0$  in  $\mathcal{S}_+$ , the function  $z$  should be a periodic coordinate with the period  $2\pi R_0$  on  $\mathcal{S}_+$ . Since  $z$  is extended so that the function on  $\mathcal{M}$ ,  $z$  should be a periodic coordinate with the period  $2\pi R_0$  also on  $\mathcal{S}_-$ . Thus the initial surface  $\mathcal{S}$  is closed and locally flat except  $\mathcal{P}$ . Further, we can easily see that the case  $\kappa_- = -1$  is equivalent to the case  $\kappa_- = 0$  by the replacement  $\mathcal{M}_- \leftrightarrow \mathcal{M}_+$ .

The initial acceleration of the wall, in this case, is

$$\left(\frac{d^2 R}{d\tau^2}\right)_0 = \frac{\lambda}{2}, \quad (4.8)$$

i.e., the domain wall begins to expand.

Thus, domain walls on momentarily static, radiation free, and regular initial configuration have the finite acceleration and do begin to move in both case in the next moment. The case in Sec.IV A 1 has the counter part in a test wall system as seen in Appendix C, while the case in Sec.IV A 2 does not. Henceforth, we concentrate on the case in Sec.IV A 1 to compare the self-gravitating wall with the test wall.

## B. Einstein-Rosen wave emission

Here, we consider the infinitesimal time evolution from the momentarily static and radiation free initial configuration in Sec.IV A 1. We separate the causal future  $J(\mathcal{S})$  of  $\mathcal{S}$  in  $\mathcal{M}$  into three pieces: the future domains of dependence  $D^+(\mathcal{S}_\pm)$  of  $\mathcal{S}_\pm$  and the causal future  $J(\mathcal{P})$  of  $\mathcal{P}$ . (See Fig.1.) We may treat these three pieces, separately. Since the initial configurations on  $\mathcal{S}_\pm$  are momentarily static and radiation free,  $D^+(\mathcal{S}_\pm)$  is still static and the metric on  $D^+(\mathcal{S}_\pm)$  is also given by Eqs.(3.2). Then, we may consider the time evolution from  $\partial J(\mathcal{P})$ .

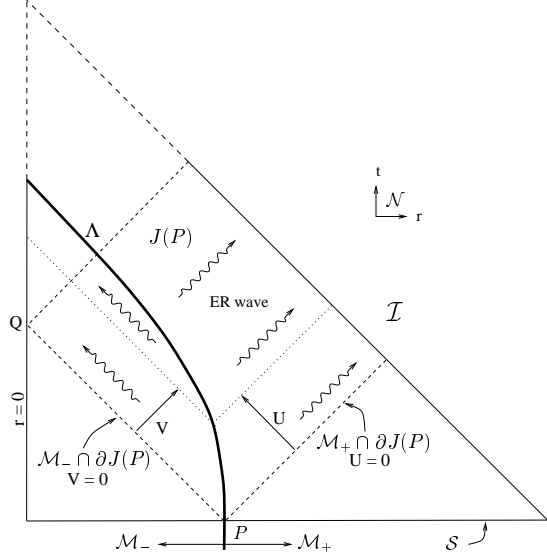


FIG. 1. The schematic picture of the orbit space  $\mathcal{N}$ . To clarify the time evolution from the initial surface  $\mathcal{S}$ , we should consider the causal future  $J(\mathcal{P})$  of  $\mathcal{P}$  and  $J(\mathcal{S}) \setminus J(\mathcal{P})$ , separately.

To consider the evolution from  $\partial J(\mathcal{P}) \cap \mathcal{M}_+$  into  $J(\mathcal{P}) \cap \mathcal{M}_+$ , we introduce the null coordinate  $U = t_+ - r + R_0$  so that  $U = 0$  at  $\partial J(\mathcal{P}) \cap \mathcal{M}_+$ . In the coordinates  $(U, r)$ , the wave equation (2.2) is given by

$$\left(2\partial_r + \frac{1}{r}\right) \partial_U \psi - \left(\partial_r^2 + \frac{1}{r}\partial_r\right) \psi = 0. \quad (4.9)$$

Since we only consider the infinitesimal time evolution from  $\partial J(\mathcal{P}) \cap \mathcal{M}_+$ , we use the Taylor expansion of solution  $\psi = \psi_+$  around  $\partial J(\mathcal{P}) \cap \mathcal{M}_+$  as follows:

$$\psi_+ = \frac{1}{\sqrt{r}} \sum_{n=0}^{\infty} \frac{1}{n!} \varphi_+^{(n)} (\omega U)^n, \quad (4.10)$$

$$\varphi_+^{(0)} = -\kappa_+ \sqrt{r} \ln(r/R_0), \quad (4.11)$$

$$\varphi_+^{(n)} = \sum_{l=0}^{n-1} a_{n-l}^+ \frac{((2l-1)!!)^2}{l!} \left(\frac{-1}{8\omega r}\right)^l \quad \text{for } n > 0, \quad (4.12)$$

where  $a_n^+$  are constants determined by the junction condition and  $\omega^{-1}$  is an appropriate time scale. We have

used the fact that the metric in the region  $D^+(\mathcal{S}_+)$  is given by Eqs.(3.2) to determine  $\varphi_+^{(0)}$ .

Similarly, in  $\mathcal{M}_-$ , we expand  $\psi$  by the advanced time interval  $V = t_- + r - R_0$  from  $\partial J(\mathcal{P}) \cap \mathcal{M}_-$ . The solution  $\psi_-(V, r)$  is obtained as follows:

$$\psi_- = \frac{1}{\sqrt{r}} \sum_{n=0}^{\infty} \frac{1}{n!} \varphi_-^{(n)} (\omega V)^n, \quad (4.13)$$

$$\varphi_-^{(0)} = 0, \quad (4.14)$$

$$\varphi_-^{(n)} = \sum_{l=0}^{n-1} a_{n-l}^- \frac{((2l-1)!!)^2}{l!} \left(\frac{1}{8\omega r}\right)^l, \quad \text{for } n > 0, \quad (4.15)$$

where  $a_n^-$  are the constants, which are determined by the junction condition (2.11).

Here, we consider the behavior of the solutions  $\psi_+$  at  $r \rightarrow \infty$ . Let  $\mathcal{I}$  denotes the asymptotic region where  $r \rightarrow \infty$  with a fixed  $U > 0$ . (See Fig.1). The asymptotic form of  $\psi_+$  at  $\mathcal{I}$  is

$$\psi_+ = -\kappa_+ \ln \frac{r}{R_0} + \frac{1}{\sqrt{r}} \sum_{n=1}^{\infty} \frac{a_n^+ (\omega U)^n}{n!} + O\left(\frac{1}{r^{3/2}}\right). \quad (4.16)$$

The first term in Eq.(4.16) is the static potential produced by the wall and the second term is the outgoing ER wave. Eq.(4.16) shows  $a_n^+$  correspond to the amplitude of the ER wave at infinity ( $r \rightarrow \infty$ ). Actually, the energy loss by the ER wave emission is estimated by the quasi-local energy introduced by Thorne [15]:

$$E = \frac{\gamma}{4G}, \quad (4.17)$$

which called “C-energy”. The energy loss is estimated by

$$\partial_U E_\infty(U) := \lim_{r \rightarrow \infty} \partial_U E(r, U). \quad (4.18)$$

Using Eqs.(2.4) and (4.16), we obtain

$$\partial_U E_\infty(U) = -\frac{1}{2G} \left( \sum_{n=1}^{\infty} \frac{a_n^+ \omega^n U^{n-1}}{(n-1)!} \right)^2. \quad (4.19)$$

It shows that the C-energy must decrease due to the outgoing ER wave ( $\partial_U E_\infty < 0$ ).

On the other hand,  $\psi_-$  given by Eqs.(4.13)-(4.15) has singular behavior at the axis  $r = 0$ . This singular behavior is removed if the superposition of the reflecting waves at  $r = 0$  is taken into account. Let  $Q$  be the point where the characteristics  $\partial J(\mathcal{P}) \cap \mathcal{M}_-$  and the world line of the axis  $r = 0$  intersects. (See Fig.1.) The reflected waves emerge at the point  $Q$  and the waves propagate into the causal future  $J(Q)$  of  $Q$ . Thus, the solution  $\psi_-$  given by Eqs.(4.13)-(4.15) is applicable in the region  $(J(\mathcal{P}) \setminus J(Q)) \cap \mathcal{M}_-$ .

Now, we determine the coefficients  $a_n^\pm$  by imposing the junction conditions. The junction conditions (2.6) and (2.11) are equivalent to the set of equations at  $\mathcal{P}$ :

$$D_{\parallel}^{n+1}[D_{\perp}\psi] = 0, \quad D_{\parallel}^n[\psi] = 0, \quad \text{for } n \geq 0. \quad (4.20)$$

After some calculations (see Appendix B), we obtain

$$a_1^\pm = 0, \quad (4.21)$$

$$\omega^2 a_2^\pm = \pm \frac{\kappa_+}{2(u_{\pm}^t)^2 \sqrt{R_0}} \left( \frac{d^2 R}{d\tau^2} \right)_0, \quad (4.22)$$

$$\begin{aligned} \omega^3 a_3^\pm &= \frac{\kappa_+}{2(u_{\pm}^t)^3 \sqrt{R_0}} \left\{ \pm \left( \frac{d^3 R}{d\tau^3} \right)_0 - \left( \frac{d^2 u_{\pm}^t}{d\tau^2} \right)_0 \right. \\ &\quad \left. + \frac{u_{\pm}^t}{R_0} \left( \frac{d^2 R}{d\tau^2} \right)_0 \right\} \pm \frac{3\omega^2 a_2^\pm}{(u_{\pm}^t)^2} \left( \frac{d^2 R}{d\tau^2} \right)_0 \\ &\quad \pm \frac{\omega^2 a_2^\pm}{8R_0} - \frac{1}{4R_0(u_{\pm}^t)^3} [(u_+^t)^3 \omega^2 a_2^+ - (u_-^t)^3 \omega^2 a_2^-], \end{aligned} \quad (4.23)$$

where all quantities in right hand side of Eqs.(4.21)-(4.23) are evaluated at  $\mathcal{P}$  and explicit form of  $(d^2 u_{\pm}^t/d\tau^2)_0$  is given by Eq.(B12) in Appendix B.

Eq.(4.22) shows that the ER wave emission is due to the wall motion  $(d^2 R/d\tau^2)_0$  in the leading order. Eq.(4.22) includes two effects in ER wave emission. First,  $\kappa_+$  plays a role of the source of ER wave. As seen in Appendix B, this comes from the difference between  $\partial_r \psi_{\pm}$  on  $\mathcal{S}$ . Second, the amplitude of the ER wave depends on  $u_{\pm}^t = e^{-\gamma_{\pm}}$ , which represents the scale difference of the proper time  $\tau$  and the time coordinate  $t_{\pm}$  (or  $U$ ) on  $\mathcal{S}_{\pm}$ . These two effects caused by the self-gravity of the wall. Eq.(4.23) contains the influence due to the ER wave emission in the next moment through Eq.(4.22).

Differentiating Eq.(2.10) with respect to  $\tau$ , we obtain

$$\left( \frac{d^3 R}{d\tau^3} \right)_0 = - \frac{2\kappa_+(u_+^t)^3}{(1-u_+^t)\sqrt{R_0}} \omega^2 a_2^+ \quad (4.24)$$

$$= \frac{\lambda(2-3\lambda R_0)}{4R_0(1-2\lambda R_0)}. \quad (4.25)$$

where we used Eqs.(B2), (4.1), (4.2), (4.4) and (4.22). As seen in Appendix C,  $(d^3 R/d\tau^3)_0$  vanishes for the test wall in Minkowski spacetime. The appearance of  $(d^3 R/d\tau^3)_0$ , which depends on the amplitude  $a_2^+$  of outgoing ER wave, arises from the back reaction of ER emission. Since  $(d^3 R/d\tau^3)_0$  has the opposite sign to the acceleration, the back reaction of ER wave emission diminishes the absolute value of the wall acceleration in this order.

Let  $\tau_b$  be the time scale where the back reaction becomes efficient, which is estimated by  $|(d^3 R/d\tau^3)_0 \tau_b| \sim |(d^2 R/d\tau^2)_0|$ . From Eqs.(4.4) and (4.25), we found

$$\tau_b \sim \frac{2(1-2\lambda R_0)}{\lambda}. \quad (4.26)$$

In the strong gravity limit  $\lambda R_0 \rightarrow 1/2$ ,  $\tau_b$  shows that the radiation reaction becomes efficient immediately. On the

other hand, in the weak gravity limit  $\lambda R_0 \ll 1$ , Eqs.(4.4) and (4.26) are given by

$$\left( \frac{d^2 R}{d\tau^2} \right)_0 \sim -\frac{1}{R_0}, \quad \tau_b \sim \frac{2}{\lambda}. \quad (4.27)$$

The initial acceleration in the weak gravity limit coincides with that of the test wall (see Appendix C). The collapsing time scale  $\tau_c$  is estimated by  $|(d^2 R/d\tau^2)|(\tau_c)^2/2 \sim R_0$ . Then we obtain  $\tau_c \sim R_0 \ll 2/\lambda \sim \tau_b$  in the same limit. Thus, in the weak gravity limit, the domain wall collapses to  $R = 0$  before the radiation reaction becomes efficient.

Substituting Eqs.(4.22) and (4.23) into Eq.(4.19), we estimate the energy loss rate of the system by the ER wave emission:

$$\partial_U E_{\infty} \sim -\frac{1}{2G} a_{2+}^2 \omega^4 U^2 \left( 1 + \frac{\omega^3 a_3^+}{\omega^2 a_2^+} U \right), \quad (4.28)$$

$$\begin{aligned} &= -\frac{1}{32G} \frac{\lambda^2(2-3\lambda R_0)^2}{(1-2\lambda R_0)^6 R_0} U^2 \times \\ &\quad \left( 1 - \frac{11-14\lambda R_0-28(\lambda R_0)^2+40(\lambda R_0)^3}{8R_0(1-2\lambda R_0)^2} U \right). \end{aligned} \quad (4.29)$$

Eq.(4.29) shows that the larger energy are carried by ER wave, as the initial total mass of the wall is larger in the leading order. A cylindrical domain wall with large total mass produces strong gravitational field and large energy density of the ER wave emitted.

In the weak gravity limit, Eq.(4.29) is given by

$$\partial_U E_{\infty} \sim -\frac{\lambda^2 U^2}{8GR_0} \left( 1 - \frac{11U}{8R_0} \right). \quad (4.30)$$

This shows that Eq.(4.30) is valid until  $U \sim 8R_0/11$  in the weak gravity limit.

## V. SUMMARY AND DISCUSSION

In summary, we have considered the spacetime with a self-gravitating cylindrical domain wall using the thin wall approximation. We considered two classes of solutions, separately, solutions with and without gravitational waves emission. First, we found two subclasses of solutions without gravitational wave emission: static wall solutions and dynamically moving wall solutions. The spacetimes that are described by the solutions have singularities inevitably. Next, we set up momentarily static and radiation free initial configurations of the system. We found that  $0 < \text{“wall’s mass per unit proper length”} < 1/(4G)$  should hold initially for regular initial configurations. In the exceptional case of  $\text{“wall’s mass per unit proper length”} = 1/(2G)$ , we found that the initial surface is closed radially. In these two regular initial configurations, the domain wall has non-vanishing initial acceleration.

We also considered the time evolution from the above initial data within the infinitesimal time interval. By the accelerated motion of the wall, ER wave emission does occur. And the wave emission affects the wall motion in the next moment. This is just the radiation reaction problem. In contrast to the test wall motion in Minkowski spacetime, the radiation reaction diminishes the acceleration of the wall. We also found that the amplitude of the emitted wave depends on the gravitational potential produced by the wall on the initial surface. Further, the back reaction of the wave emission to the wall motion depends both on the amplitude of the wave and on the gravitational potential. As the result, a cylindrical domain wall with the large initial mass produces the large gravitational potential. The wall motion in the large potential yields the large amount of the ER wave. By this strong ER wave emission the large back reaction to the wall motion does occur.

Here, we compare the motion of the self-gravitating wall with that of the test wall. When  $\lambda R_0 \ll 1$ , the back reaction to the wall motion by ER wave emission is negligible since the wall collapse to  $r = 0$  before the back reaction becomes significant. Then, when  $\lambda R_0 \ll 1$ , the motion of a self-gravitating wall is well approximated by those of test walls. In the weak gravity limit, the energy loss rate by ER wave emission is estimated from Eq.(4.30). Since the collapsing time scale is given by  $U \sim R_0$ , the energy loss rate per length along  $z$  direction is

$$\partial_u E_\infty \sim -2\pi^2 G \sigma^2 R_0. \quad (5.1)$$

Though Eq.(4.30) is not valid when  $U \sim 8R_0/11$ , we have extrapolated it. We note that the energy loss rate (5.1) does agree with that roughly estimated from the quadrupole formula for gravitational wave emission. This is our main conclusion in this paper.

The results obtained here are quite reasonable and these are expected from the behavior of the test Nambu-Goto wall in the absence of their self-gravity. However, the behaviors of gravitating Nambu-Goto membranes obtained in Refs. [7,8] are different from those of test membranes. We must note that the behavior similar to that in Refs. [7,8] is also obtained in the ER wave scattering by the cylindrical domain wall in the static background as seen in Appendix D, i.e., there is no solution which corresponds to the spontaneous oscillation of the wall. Further, we see that the cylindrical domain wall considered in Appendix D is unstable. The unstable mode is not oscillatory mode. Though our analysis in Appendix D is restricted to the perturbation of ER wave, we expect that the oscillatory behavior of the wall, the oscillatory behavior is same as those in Refs. [7,8].

Together with the results from some models in Refs. [7,8] and in this paper, we conjecture that the oscillatory motion of test walls fails to approximate that of a self-gravitating wall, but monotonically collapsing motions of the self-gravitating wall are well approximated

by those of the test wall if its energy density is sufficiently small. Further, the energy of gravitational waves emitted by monotonic motions of the walls is estimated by the quadruple formula.

Of course, in the dynamics of domain walls in the realistic situation in the early universe, the effective equation of state of an oscillating wall may change, analogous to that of the wiggling cosmic string [1]. This is pointed out by Bonjour et.al [16]. This change will be the effect to be taken into account when we discuss the dynamics of domain walls in the realistic situation in the early universe. However, we should emphasize that our discussion is concentrated on the difference between the oscillatory behavior of a gravitating Nambu-Goto membrane and a test Nambu-Goto membrane. At least, the oscillatory behavior of gravitating Nambu-Goto membranes is quite different from that of test membranes, while monotonically collapsing motion is well approximated by the test membranes. This suggests that the energy of gravitational waves estimated by the oscillating test membranes might be incorrect. Though the full dynamics of gravitating Nambu-Goto membranes is not clear yet, to estimate the energy of gravitational waves from defects, we should clarify the dynamics of Nambu-Goto membranes at first. After that, the effect of the change in the equation of state should be included. Though the gravitational waves might be emitted by this change, this physical process is different from that discussed here.

## ACKNOWLEDGMENTS

The author would like to thank H. Ishihara, T. Okamura, A. Ishibashi, K. Nakao and T. Mishima for valuable comments and discussions. The author also thanks to M. Tachiki, M. Date and M. Omote for their encouragement.

## APPENDIX A: WEYL CANONICAL FORM AND STRONG GRAVITY LIMIT

As mentioned in the main text, the cylindrically symmetric spacetime we considered here is characterized by the existence of two commutable spacelike Killing vectors, which are both hypersurface orthogonal. In this Appendix, we explicitly see that the metric on this spacetime is reduced to Eq.(2.1) using the Einstein equation even if the wall exists.

The metric on the spacetime which has two hypersurface orthogonal Killing vectors  $(\partial/\partial\phi)^a$  and  $(\partial/\partial z)^a$  is given by

$$ds^2 = g_{ab} dx^a dx^b = e^{2\psi} dz^2 + e^{-2\psi} (\beta^2 d\phi^2 + f_{ab} d\bar{x}^a d\bar{x}^b), \quad (A1)$$

where  $f_{ab}$  is the two dimensional Lorentzian metric ( $f_{ab}(\partial/\partial z)^a = f_{ab}(\partial/\partial\phi)^a = 0$ ), and  $f_{ab}$ ,  $\psi$  and  $\beta$  depend only on the two dimensional coordinates  $\bar{x}^a$ .  $e^\psi$



and  $e^{-\psi}\beta$  are the norms of the Killing vector  $z^a$  and  $\phi^a$ , respectively.

By choosing an appropriate null coordinates,  $f_{ab}$  in Eq.(A1) is written by the conformal flat form without loss of generality:

$$f_{ab}d\bar{x}^a d\bar{x}^b = -e^{2\bar{\gamma}}dx^+ dx^-. \quad (\text{A2})$$

When one treat the cylindrical vacuum spacetime, the function  $\beta$  is constrained by one of the components of the Einstein equations,  $R_z^z + R_\phi^\phi = 0$  ( $R_\phi^a$  is the Ricci tensor), which yields

$$\partial_{x^+}\partial_{x^-}\beta = 0. \quad (\text{A3})$$

The general solution to this equation is

$$\beta = f_1(x^+) + f_2(x^-), \quad (\text{A4})$$

where  $f_1(x^+)$  and  $f_2(x^-)$  are arbitrary functions of  $x^+$  and  $x^-$ , respectively. The gradient of  $\beta$  determines whether we may choose  $\beta$  as a spatial coordinate or not. Actually, when  $\partial_a\beta$  is spacelike, we may introduce new null coordinates  $\bar{u}$  and  $\bar{v}$  so that  $\beta = (\bar{u} - \bar{v})/2$ , and new coordinates  $t$  and  $r$  by  $t = (\bar{u} + \bar{v})/2$  and  $r = (\bar{u} - \bar{v})/2$ . Hence, one may perform the conformal transformation on the  $(x^+, x^-)$  plane to  $(t, r)$  plane so that  $\beta = r$ . Thus, we have the Weyl canonical form (2.1).

We must note that the signature of  $\partial_a\beta$  is determined whether  $\beta$  should be chosen by the spatial coordinate or not. When  $\partial_a\beta$  is timelike or null,  $\beta$  should be regarded as the time or null coordinate, respectively. Further, we also note that the signature of  $\partial_a\beta$  also depends on the Einstein equation. It is not trivial whether above reduction is valid when the wall exists. Here, we show that we may choose  $\beta$  as the radial coordinate on the momentarily static initial surface when  $\lambda R_0 \neq 1/2$ .

We only consider the case  $\partial_a\beta$  is spacelike in  $\mathcal{M}_-$ . In the coordinate system (A1), one of the junction conditions is reduced to

$$[D_\perp\beta] = -2\lambda\beta. \quad (\text{A5})$$

The condition (A5) corresponds to Eq.(2.12) in the main text. Using the condition (A5), we have

$$\begin{aligned} [\partial_a\beta\partial^a\beta] &= [-(D_\parallel\beta)^2 + (D_\perp\beta)^2] \\ &= -4((D_\perp\beta)_- - \lambda\beta)\lambda\beta, \end{aligned} \quad (\text{A6})$$

and

$$(\partial_a\beta\partial^a\beta)_+ = -((D_\parallel\beta)_-)^2 + ((D_\perp\beta)_- - 2\lambda\beta)^2. \quad (\text{A7})$$

Since we choose  $\beta = r$  on  $\mathcal{S} \cap \mathcal{M}_-$ , we have  $D_\parallel\beta = 0$  and  $D_\perp\beta = 1$  on  $\mathcal{S} \cap \mathcal{M}_-$ . Then we can see that  $(\partial_a\beta)_+$  is spacelike when  $\lambda\beta \neq 1/2$ .

When  $\lambda\beta = 1/2$ ,  $(\partial_a\beta)_+$  is null or zero. Note that the case  $\lambda\beta = 1/2$  corresponds to the ‘‘strong gravity limit’’ in the main text. This geometry is obtained by taking limit  $\kappa \rightarrow \infty$  in the metric (3.3). Using the proper radial

coordinate defined by (4.5), we see that  $g_{tt}$ ,  $g_{zz}$  and  $g_{\phi\phi}$  behave

$$g_{tt} \sim \kappa^4 \left(\frac{\rho}{R_0}\right)^2, \quad g_{zz} \sim 1, \quad g_{\phi\phi} \sim R_0^2. \quad (\text{A8})$$

in the limit  $\kappa \rightarrow \infty$ . Hence, the metric (3.3) is given by

$$ds^2 = -\rho^2 dT^2 + d\rho^2 + dz^2 + R_0^2 d\phi^2. \quad (\text{A9})$$

This metric means  $\mathcal{S}_+$  is locally flat but the circumference of symmetric cylinder is constant  $2\pi R_0$  outward as mentioned in the main text. This metric shows that  $\partial_a\beta$  is zero. This corresponds to the choice  $\beta = R_0$ , where  $R_0$  is the initial locus of the wall. This choice is required by the junction condition (2.6).

## APPENDIX B: INFINITESIMAL TIME EVOLUTION OF ER WAVE

In this appendix, we show the derivation of (4.21)-(4.23). Only we have to do is to evaluate the junction conditions (2.6) and (2.11) for arbitrary  $\tau$  and determine  $a_{n\pm}$ . Since we set up the momentarily static initial configuration, which satisfy  $\partial_t\psi = 0$ , i.e.,  $a_{1\pm} = 0$ .  $a_n^\pm$  for  $n \geq 1$  are determined by the evaluation of (4.20) at  $\mathcal{P}$ . We consider the cases  $(\epsilon_-, \epsilon_+) = (+, \pm)$ , separately.

### 1. $(\epsilon_-, \epsilon_+) = (+, +)$ case

To evaluate (4.20) for this case, it is convenient to use the following representations of  $D_\parallel$  and  $D_\perp$ ;

$$\begin{aligned} D_{\parallel+} &= (u_+^t - u^r)\partial_U + u^r\partial_r, \\ D_{\perp+} &= (u^r - u_+^t)\partial_U + u^t\partial_r, \\ D_{\parallel-} &= (u_-^t + u^r)\partial_V + u^r\partial_r, \\ D_{\perp-} &= (u^r + u_-^t)\partial_V + u^t\partial_r. \end{aligned} \quad (\text{B1})$$

Further, when we evaluates (4.20) at  $\mathcal{P}$ , the momentarily static condition  $u^r = \dot{u}_\pm^t = 0$  are used. Note that  $d^n u^r/d\tau^n \neq 0$  and  $d^{n+1} u_\pm^t/d\tau^{n+1} \neq 0$  for  $n \geq 2$ . It is also convenient to use the expression

$$\begin{aligned} \partial_r^n \partial_U^m \psi_{\mathcal{P}+} &= \omega^m \partial_r^n \left( \frac{\varphi_+^{(m)}}{\sqrt{r}} \right) \Bigg|_{r=R_0}, \\ \partial_r^n \partial_V^m \psi_{\mathcal{P}-} &= \omega^m \partial_r^n \left( \frac{\varphi_-^{(m)}}{\sqrt{r}} \right) \Bigg|_{r=R_0}. \end{aligned} \quad (\text{B2})$$

Here, the subscript ‘‘ $\mathcal{P}+$ ’’ means the evaluation at  $U = +0$  and  $r = R_0 + 0$  and ‘‘ $\mathcal{P}-$ ’’ means the evaluation at  $V = +0$  and  $r = R_0 - 0$ .

The junction conditions (4.20) with  $n = 2$  are given by

$$\omega^2(u_+^t)^2\varphi_+^{(2)} + \omega^2(u_-^t)^2\varphi_-^{(2)} = 0, \quad (\text{B3})$$

$$\begin{aligned} & \omega^2(u_+^t)^2\varphi_+^{(2)} - \omega^2(u_-^t)^2\varphi_-^{(2)} \\ &= -\sqrt{r}\dot{u}^r \left( \partial_r \left( \frac{\varphi_+^{(0)}}{\sqrt{r}} \right) - \partial_r \left( \frac{\varphi_-^{(0)}}{\sqrt{r}} \right) \right) \Big|_{r=R_0}. \end{aligned} \quad (\text{B4})$$

Then we obtain

$$\begin{aligned} & \omega^2(u_\pm^t)^2\varphi_\pm^{(2)} \\ &= \mp \frac{\sqrt{r}}{2}\dot{u}^r \left( \partial_r \left( \frac{\varphi_\pm^{(0)}}{\sqrt{r}} \right) - \partial_r \left( \frac{\varphi_\mp^{(0)}}{\sqrt{r}} \right) \right) \Big|_{r=R_0}. \end{aligned} \quad (\text{B5})$$

Since  $\varphi_\pm^{(0)}/\sqrt{r} = -\kappa_\pm \ln(r/R_0)$  and  $\kappa_+ \neq \kappa_-$  from the regularity of the initial configuration,  $\varphi_\pm^{(2)}$  does not vanishes, i.e., the ER wave emission occurs by the wall motion. When  $\kappa_- = 0$ , Eq.(B5) gives Eq.(4.22) by substituting  $\varphi_+^{(0)} = -\kappa_+\sqrt{r}\ln(r/R_0)$ .

The conditions (4.20) with  $n = 3$  are given by

$$\begin{aligned} & \omega^3(u_+^t)^3\varphi_+^{(3)} + \omega^3(u_-^t)^3\varphi_-^{(3)} \\ &= 3\dot{u}^r \left( u_+^t\omega^2\varphi_+^{(2)} - u_-^t\omega^2\varphi_-^{(2)} \right) \\ &+ \sqrt{r}\dot{u}^r \left( u_+^t\partial_r^2 \left( \frac{\varphi_+^{(0)}}{\sqrt{r}} \right) - u_-^t\partial_r^2 \left( \frac{\varphi_-^{(0)}}{\sqrt{r}} \right) \right) \\ &+ \sqrt{r} \left( (u_+^t)^3\omega^2\partial_r \left( \frac{\varphi_+^{(2)}}{\sqrt{r}} \right) - (u_-^t)^3\omega^2\partial_r \left( \frac{\varphi_-^{(2)}}{\sqrt{r}} \right) \right) \\ &+ \sqrt{r} \left( \ddot{u}_+^t\partial_r \left( \frac{\varphi_+^{(0)}}{\sqrt{r}} \right) - \ddot{u}_-^t\partial_r \left( \frac{\varphi_-^{(0)}}{\sqrt{r}} \right) \right) \Big|_{r=R_0}, \quad (\text{B6}) \\ & (u_+^t)^3\psi_+^{(3)} - (u_-^t)^3\psi_-^{(3)} \\ &= 3\dot{u}^r \left( u_+^t\omega^2\varphi_+^{(2)} + u_-^t\omega^2\varphi_-^{(2)} \right) \\ &- \sqrt{r}\dot{u}^r \left( \partial_r \left( \frac{\varphi_+^{(0)}}{\sqrt{r}} \right) - \partial_r \left( \frac{\varphi_-^{(0)}}{\sqrt{r}} \right) \right) \Big|_{r=R_0}. \quad (\text{B7}) \end{aligned}$$

Then we obtain

$$\begin{aligned} & \omega^3(u_\pm^t)^3\varphi_\pm^{(3)} \\ &= \pm 3\dot{u}^r u_\pm^t\omega^2\varphi_\pm^{(2)} \mp \frac{\sqrt{r}}{2}\ddot{u}^r \left( \partial_r \left( \frac{\varphi_\pm^{(0)}}{\sqrt{r}} \right) - \partial_r \left( \frac{\varphi_\mp^{(0)}}{\sqrt{r}} \right) \right) \\ &+ \frac{\sqrt{r}}{2}\dot{u}^r \left( u_+^t\partial_r^2 \left( \frac{\varphi_+^{(0)}}{\sqrt{r}} \right) - u_-^t\partial_r^2 \left( \frac{\varphi_-^{(0)}}{\sqrt{r}} \right) \right) \\ &+ \frac{\sqrt{r}}{2} \left( (u_+^t)^3\omega^2\partial_r \left( \frac{\varphi_+^{(2)}}{\sqrt{r}} \right) - (u_-^t)^3\omega^2\partial_r \left( \frac{\varphi_-^{(2)}}{\sqrt{r}} \right) \right) \\ &+ \frac{\sqrt{r}}{2} \left( \ddot{u}_+^t\partial_r \left( \frac{\varphi_+^{(0)}}{\sqrt{r}} \right) - \ddot{u}_-^t\partial_r \left( \frac{\varphi_-^{(0)}}{\sqrt{r}} \right) \right) \Big|_{r=R_0}. \end{aligned} \quad (\text{B8})$$

When  $\kappa_- = 0$ , Eq.(B8) gives Eq.(4.23) by substituting  $\varphi_+^{(0)} = -\kappa_+\sqrt{r}\ln(r/R_0)$ .

Finally,  $\ddot{u}_\pm^t$  in (B7) for the case in Sec.IV A 1 is derived as follows: Consider the norm condition of  $u^a$ :

$$(u_+^t)^2 = (u^r)^2 + e^{-2(\Gamma_+ - \Psi)}. \quad (\text{B9})$$

Differentiating (B9) and using the momentarily static conditions  $u^r = \dot{\Psi} = \dot{\Gamma} = 0$  and  $\Psi = 0$  at  $\mathcal{P}$ , we obtain

$$u_+^t\ddot{u}_+^t = \ddot{R}^2 - (\ddot{\Gamma}_+ - \ddot{\Psi})e^{-2\Gamma_+}. \quad (\text{B10})$$

By virtue of (2.3), (2.4), (4.10) and (B2), we obtain

$$\begin{aligned} \ddot{\Gamma}_+ - \ddot{\Psi} &= \frac{\kappa_+(\kappa_+ + 1)}{R_0}\dot{u}^r \\ &- (2\kappa_+ + 1)(u_+^t)^2 \frac{\omega^2}{\sqrt{R_0}}\varphi_+^{(2)}. \end{aligned} \quad (\text{B11})$$

Then (B10) gives

$$\begin{aligned} \ddot{u}_{+0}^t &= \frac{1}{u_+^t} \left( \frac{d^2R}{d\tau^2} \right)_0 - \frac{\kappa_+(\kappa_+ + 1)}{R_0}u_+^t \left( \frac{d^2R}{d\tau^2} \right)_0 \\ &+ (2\kappa_+ + 1)(u_+^t)^3 \frac{\omega^2 a_2^+}{\sqrt{R_0}}. \end{aligned} \quad (\text{B12})$$

## 2. $(\epsilon_-, \epsilon_+) = (+, -)$ case

In this case, in both  $\mathcal{M}_\pm$ , ER wave propagates to the direction along which the radial function  $r$  decreases. Then, we should use

$$\psi_+ = \frac{1}{\sqrt{r}} \sum_{n=0}^{\infty} \frac{1}{n!} \varphi_+^{(n)} (\omega V_+)^n, \quad (\text{B13})$$

$$\varphi_+^{(0)} = \ln \left( \frac{r}{R_0} \right), \quad (\text{B14})$$

$$\varphi_+^{(n)} = \sum_{l=0}^{n-1} a_{n-l}^+ \frac{((2l-1)!!)^2}{l!} \left( \frac{1}{8\omega r} \right)^l, \quad \text{for } n > 0, \quad (\text{B15})$$

as the solution to (2.2) in  $J(\mathcal{P}) \cap \mathcal{M}_+$ , where  $V_+ = t_+ + r - R_0$ . Further, the representations of  $D_{\parallel}$  and  $D_{\perp}$  are given by

$$\begin{aligned} D_{\parallel+} &= (u_+^t + u^r)\partial_{V_+} + u^r\partial_r, \\ D_{\perp+} &= -(u^r + u_+^t)\partial_{V_+} - u^t\partial_r, \\ D_{\parallel-} &= (u_-^t + u^r)\partial_{V_-} + u^r\partial_r, \\ D_{\perp-} &= (u^r + u_-^t)\partial_{V_-} + u^t\partial_r, \end{aligned} \quad (\text{B16})$$

where  $V_- = V = t_- + r - R_0$ .

The evaluations for (4.20) with  $n = 2$  by the similar calculations to the case  $(\epsilon_-, \epsilon_+) = (+, +)$  give the same form as (B5). Since  $\varphi_+^{(0)}/\sqrt{r} = \ln(r/R_0)$  and  $\varphi_-^{(0)} = 0$ , the ER wave emission occurs by the wall motion. Furthermore, it is straight forward to obtain  $\varphi_\pm^{(3)}$  by the evaluation of (4.20) with  $n = 3$ .

## APPENDIX C: DYNAMICS OF CYLINDRICAL TEST WALL

We consider the test wall motion with the cylindrical symmetry for comparison with the motion of the self-gravitating wall in the main text. The test wall motion is given by  $K = 0$ , where  $K$  is the trace of the extrinsic curvature of the wall world volume. For a cylindrical test wall in Minkowski spacetime, the equation of motion is given by

$$\frac{d^2 R}{d\tau^2} + \frac{1}{R} \left( \left( \frac{dR}{d\tau} \right)^2 + 1 \right) = 0. \quad (\text{C1})$$

The solution to this equation is

$$R = \sqrt{R_0^2 - \tau^2} \sim R_0 - \frac{1}{2} \frac{\tau^2}{R_0} + R_0 O \left( \left( \frac{\tau}{R_0} \right)^4 \right). \quad (\text{C2})$$

The time symmetric initial surface is at  $\tau = 0$  and the acceleration of the wall and the third derivative of  $R$  at  $\tau = 0$  are given by

$$\left( \frac{d^2 R}{d\tau^2} \right)_0 = -\frac{1}{R_0}, \quad \left( \frac{d^3 R}{d\tau^3} \right)_0 = 0. \quad (\text{C3})$$

## APPENDIX D: PERTURBATIVE EINSTEIN ROSEN WAVE SCATTERING BY A CYLINDRICAL DOMAIN WALL

In this appendix, we consider the ER wave scattering by the domain wall using one of the simplest static solutions obtained in Sec.III and shows that the behavior of the wall is similar to the case of the spherical wall [7]. This spacetime is an exact solution discussed by Iper and Sikivie [5]. The whole spacetime consists of two regions with the identical Levi-Civita metric matched by the domain wall. On this background solution, we consider the perturbative ER wave and the perturbative motion of the domain wall.

First, we describe the background spacetime and the ER wave perturbation on this spacetime (Sec.D 1). Second, we show the relation of the proper time  $\tau$ , the Gaussian normal  $\chi$  of the wall, and the coordinates  $t, r$  in the main text to solve the ER wave scattering by the domain wall (Sec.D 2). Finally, we solve the scattering problem using the ‘‘high frequency approximation’’ (Sec.D 3).

As mentioned in the main text, the background solution we use here has curvature singularities. However, this singularity is not essential to our result.

### 1. Background and Perturbation

As the background spacetime, we consider the spacetime in Sec.III B with  $\gamma_{0\pm} = 0$ . The line element is given by

$$ds^2 = \sqrt{\frac{R_0}{r}} (-dt^2 + dr^2) + \frac{r}{R_0} dz^2 + R_0 r d\phi^2, \quad (\text{D1})$$

The axis  $r = 0$  are curvature singularities and the Riemann polynomial (3.5) diverge as  $R^{abcd} R_{abcd} \propto r^{-3}$  there and vanish at the infinity  $r \rightarrow \infty$ . Since the orbit space  $\mathcal{N}$  is conformally flat, the conformal diagram of  $\mathcal{N}$  has timelike, spatial and null infinities.

In the spacetime in Sec.III B with  $\gamma_{0\pm} = 0$ , the motion of the wall is determined by the equation (3.15) and the trajectory  $\Sigma \cap \mathcal{N}$  on  $\mathcal{N}$  is given by the equation:

$$\left( \frac{dr}{dt} \right)^2 + \frac{1}{\lambda^2 R_0^{1/2} r^{3/2}} - 1 = 0. \quad (\text{D2})$$

The qualitative behavior of the wall motion is as follows: Seeing from an observer whose world line is  $r = \text{constant}$  in either vacuum region, the domain wall first starts to shrink from the past null infinity at the light velocity, decelerates its speed, and bounces at a finite radius

$$r_0 := \frac{1}{\lambda^{4/3} R_0^{1/3}}. \quad (\text{D3})$$

After that it expands to the null infinity. Then the solution to (D2) is contained in the region

$$\mathcal{D} := \{ (t, r) \mid r^2 - t^2 > 0 \} \quad (\text{D4})$$

in  $\mathcal{N}$ . The resulting spacetime  $\mathcal{M}$  has the future and the past null infinities each of which has two connected components. The global structure of this spacetime is analogous to that in Ref. [7] but there are singularities at  $r = 0$ . (See Fig.2.)

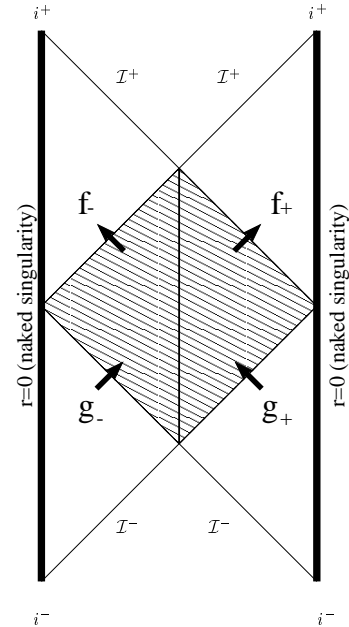


FIG. 2. The background spacetime  $\mathcal{M}$  of our scattering problem. The shaded region is  $\mathcal{D}$  defined by (D4) and  $\Sigma$  is contained in  $\mathcal{D}$ .

On this spacetime, we consider the perturbative deformation of the wall due to the scattering of the perturbative ER wave:

$$\psi = \frac{1}{2} \ln \frac{r}{R_0} + \epsilon \varphi, \quad \gamma = \frac{1}{4} \ln \frac{r}{R_0} + \epsilon \varphi, \quad (\text{D5})$$

where  $\epsilon$  is the infinitesimal parameter for the perturbation. Since the equation (2.2) is linear,  $\varphi$  is governed by the same equation as Eq.(2.2). Here we have ignored the constant term in  $\gamma$  which corresponds to the additional deficit angle around axis  $r = 0$  due to the perturbation.

To construct the global solution to  $\varphi$ , we must consider the Israel's junction condition at  $\Sigma$  for  $\varphi$ :

$$[\varphi] = 0, \quad [D_\perp \varphi] = 0. \quad (\text{D6})$$

We must also note that the junction condition (2.12) leads to the same equation of motion of the domain wall as (D2) in the order of  $O(\epsilon)$  even if we include the perturbative term  $\epsilon \varphi$ . However, the wall does undergo the quadrupole deformation by the perturbed ER wave. Actually, the circumferential radius of the domain wall along the Killing direction  $\phi^a$  is fluctuated as

$$\mathcal{R} = 2\pi \sqrt{R_0 R} (1 - \epsilon \varphi_s) \quad (\text{D7})$$

within the linear order of  $\epsilon$ , where  $\varphi_s = \varphi|_\Sigma$ . Further, the proper length along the Killing orbit of  $z^a$  is deformed as

$$e^\psi dz = \left( \sqrt{\frac{r}{R_0}} + \epsilon \varphi_s \right) dz. \quad (\text{D8})$$

Then, ER wave is directly related to the fluctuations of  $\Sigma$  and the intrinsic geometries of  $\Sigma$  are fluctuated by the perturbative ER wave  $\varphi$  if  $\varphi_s$  does not vanish. This situation is the same as that in Ref. [7].

## 2. Coordinates on $\mathcal{D}$

To solve the ER wave scattering by the domain wall, it is convenient to give the explicit relation between the coordinate system  $(t, r)$  in the Weyl canonical form (2.1) and the comoving coordinate  $(\tau, \chi)$  of the wall trajectory  $\Sigma \cap \mathcal{N}$ .

Suppose that the solution to Eq.(D2) is given by

$$v = p(u) \quad (\text{D9})$$

where  $v = t + r$  and  $u = t - r$ . The asymptotic behavior of  $p(u)$  is as follows:

$$p(u) \sim \begin{cases} \frac{1}{\lambda^2 \sqrt{R_0}} \sqrt{\frac{2}{-u}} & (u \rightarrow -\infty); \\ \frac{2}{\lambda^4 R_0 u^2} & (u \rightarrow -0). \end{cases} \quad (\text{D10})$$

Since  $\Sigma \cap \mathcal{N}$  is timelike,  $\Sigma \cap \mathcal{N} \subset \mathcal{D}$ , where

$$\mathcal{D} = \{(v, u) | 0 < v < +\infty, -\infty < u < 0\}. \quad (\text{D11})$$

Here, we introduce new double null coordinates

$$q(\sigma^+) = v, \quad q(\sigma^-) = p(u). \quad (\text{D12})$$

$q$  is a monotonically increasing function determined so that the unit normal  $n^a$  of  $\Sigma \cap \mathcal{N}$  is

$$n^a = \left( \frac{\partial}{\partial \sigma^+} \right)^a - \left( \frac{\partial}{\partial \sigma^-} \right)^a, \quad (\text{D13})$$

at least on  $\Sigma \cap \mathcal{N}$ . In terms of  $\sigma^\pm$ ,  $\Sigma \cap \mathcal{N}$  is given by  $\sigma^+ = \sigma^-$  and the metric on  $\mathcal{D}$  is given by

$$ds^2|_{\mathcal{N}} = -2g(\sigma^+, \sigma^-) d\sigma^+ d\sigma^-, \quad (\text{D14})$$

where

$$g(\sigma^+, \sigma^-) = \frac{1}{2} \sqrt{\frac{2R_0}{q(\sigma^+) - p^{-1} \circ q(\sigma^-)}} \times \frac{1}{p' \circ q(\sigma^-)} \frac{dq}{d\sigma^+}(\sigma^+) \frac{dq}{d\sigma^-}(\sigma^-). \quad (\text{D15})$$

In (D15),  $p^{-1}(v)$  is the inverse function of  $v = p(u)$ ,  $\circ$  denotes the composite function, and  $p'(v) = dp/du(u = p^{-1}(v)) = dp/du \circ p^{-1}(v)$ . Then, the monotonically increasing function  $q$  is determined by  $n^a n_a = 1$  on  $\Sigma \cap \mathcal{N}$  ( $\sigma^+ = \sigma^-$ ):

$$\frac{dq}{d\sigma^+} = \sqrt{p' \circ q(\sigma^+) \sqrt{\frac{q(\sigma^+) - p^{-1} \circ q(\sigma^+)}{2R_0}}}. \quad (\text{D16})$$

Then, the coordinate transformation from  $(u, v)$  to  $(\sigma^-, \sigma^+)$  is given by

$$\sigma^- = \int du \sqrt{p'(u) \sqrt{\frac{2R_0}{p(u) - u}}}, \quad (\text{D17})$$

$$\sigma^+ = \int dv \sqrt{\frac{1}{p' \circ p^{-1}(v)} \sqrt{\frac{2R_0}{v - p^{-1}(v)}}} \quad (\text{D18})$$

from Eqs.(D12).

From Eq.(D10), the asymptotic behaviors of the coordinates  $\sigma^\pm$  are

$$\sigma^- \sim -\frac{1}{\lambda} \ln(-u), \quad \sigma^+ \sim \frac{2}{\lambda} \ln v, \quad (u \rightarrow -\infty), \quad (\text{D19})$$

$$\sigma^- \sim -\frac{1}{\lambda} \ln(-u), \quad \sigma^+ \sim \frac{2}{\lambda} \ln v, \quad (u \rightarrow -0). \quad (\text{D20})$$

Then,  $\sigma^\pm$  is  $C^1$  function on the region  $\mathcal{D}$  and  $\mathcal{D}$  is covered by the coordinate system:

$$\mathcal{D} = \{(\sigma^+, \sigma^-) | -\infty < \sigma^\pm < \infty\}. \quad (\text{D21})$$

### 3. ER wave scattering

Using above coordinates  $\sigma^\pm$  in  $\mathcal{D}$ , we consider the scattering problem of ER wave by the cylindrical domain wall. To solve the problem, we consider the “high frequency approximation” in the region  $\mathcal{D}$ .

In terms of the null coordinates  $\sigma^\pm$ , Eq.(2.2) is given by

$$\left(-\partial_+\partial_- + \frac{1}{16r(\sigma^+, \sigma^-)^2} \frac{dv}{d\sigma^+} \frac{du}{d\sigma^-}\right) (\sqrt{r}\varphi) = 0, \quad (\text{D22})$$

where  $\partial_\pm = \partial/\partial\sigma^\pm$ . From the above construction of the coordinate system  $\sigma^\pm$ , the proper time  $\tau$  and the Gaussian normal coordinate  $\chi$  of  $\Sigma \cap \mathcal{D}(= \Sigma \cap \mathcal{N})$  are given by  $\tau = (\sigma^+ + \sigma^-)/2$ ,  $\chi = (\sigma^+ - \sigma^-)/2$ . Then, Eq.(D22) is also given by

$$(-\partial_\tau^2 + \partial_\chi^2 + V(\tau, \chi)) (\sqrt{r}\varphi) = 0, \quad (\text{D23})$$

$$V(\tau, \chi) \equiv \frac{1}{4r(\sigma^+, \sigma^-)^2} \frac{dv}{d\sigma^+} \frac{du}{d\sigma^-}. \quad (\text{D24})$$

The “high frequency approximation” considered here is as follows: Consider the Fourier decomposition of  $\varphi = \int d\omega e^{i\omega\tau} \varphi_\omega(\chi)$ . Further, we denote the maximum of the absolute value of the potential  $V(\tau, \chi)$  along  $\Sigma \cap \mathcal{D}$  by  $\|V(\tau, 0)\|$ . If  $\omega^2$  is sufficiently large,  $\omega^2 \gg \|V(\tau, 0)\|$ , we may ignore the potential term in Eq.(D23). From Eqs.(D17) and (D18), we obtain

$$\frac{du}{d\sigma^-} \frac{dv}{d\sigma^+} = \sqrt{\frac{r}{R_0}} \quad (\text{D25})$$

along the trajectory  $\Sigma \cap \mathcal{D}$  and

$$\|V(\tau, 0)\| = \frac{\lambda^2}{4}. \quad (\text{D26})$$

Here, we note that  $V(\tau, \chi)$  is maximum at the turning point (D3). Thus, the “high frequency approximation” here corresponds to the concentration on the waves with the frequency much larger than the wall tension.

In the “high frequency approximation”, the solution to the wave equation (D23) is given by

$$\varphi_\pm \sim f(\sigma^+)_{\pm} + g(\sigma^-)_{\pm}, \quad (\text{D27})$$

where  $f$  and  $g$  are arbitrary functions which satisfy the conditions

$$\partial_+^2 f \gg \frac{\lambda^2}{4} f, \quad \partial_-^2 g \gg \frac{\lambda^2}{4} g. \quad (\text{D28})$$

Evaluating the junctions conditions (D6) on  $\Sigma \cap \mathcal{D}$ , we obtain

$$f_\pm(\sigma^+) = c_\pm e^{\frac{\lambda\sigma^+}{2}} + e^{\frac{\lambda\sigma^+}{2}} \int^{\sigma^+} d\hat{\tau} \left( \frac{dg_\pm}{d\hat{\tau}} + \frac{\lambda}{2} g_\pm \right) e^{-\frac{\lambda\hat{\tau}}{2}}, \quad (\text{D29})$$

where  $g_\pm$  and  $f_\pm$  are incident and scattered wave, respectively (See Fig.2), and  $c_\pm$  are constants of integration. We note that the first term does not depend on the incident waves, while the second term of Eq.(D29) corresponds to the reflected or transmitted waves of the incident waves. The solution

$$f_\pm(\sigma^+) = c_\pm e^{\lambda\sigma^+/2} \quad (\text{D30})$$

is singular at the future boundary of the region  $\mathcal{D}$ , which does not satisfy the condition (D28). Then, within our approximation, we conclude that the domain wall does not emit gravitational waves spontaneously by its free oscillations in the high frequency approximation. This conclusion is same as those in Ref. [7].

We must note that the result obtained here does not depend on the boundary condition on the singularity  $r = 0$  of the background spacetime. Our consideration is restricted in the region  $\mathcal{D}$  and the singularity  $r = 0$  is not in  $\mathcal{D}$  but on the boundary  $\partial\mathcal{D}$  of the closure of  $\mathcal{D}$ . From the causality determined by Eq.(2.2), the singularity  $r = 0$  on  $\partial\mathcal{D}$  does not give any effects in  $\mathcal{D}$ .

We must also note the fact that the “high frequency approximation” discussed here gives exact scattering data in the model of Ref. [7] and the solution similar to Eq.(D30) is obtained. The solution obtained by this approximation is just  $k = -i$  mode in Ref. [7]. Then we may say that the solution based on the high frequency approximation is also correct beyond the validity of the approximation in the exactly solvable model in Ref. [7]. If we apply this extrapolation to the solution (D29), the only solution in the absence of incidental wave is (D30) and we conclude that the background cylindrical domain wall considered here is unstable.

- 
- [1] A. Vilenkin and E.P.S Shellard, “*Cosmic Strings and Other Topological Defects*”, (Cambridge University Press, Cambridge, England, 1994).
  - [2] E.W. Kolb and M.S. Turner, *The Early Universe*, (Addison-Wesley Publishing Company, 1993). T.W.B Kibble, Phys. Rep. **67** (1980), 183. T. Vachaspati, Nucl. Phys. B **277**, 593, (1986). M. Sakellariadou, Phys. Rev. D **42**, 354, (1990). R.R.. Caldwell and B. Allen, *ibid.*, **45**, 3447, (1992). P. Casper and B. Allen, *ibid.*, **52**, 4337, (1995). Publishing Company, 1993) and its references therein.
  - [3] A. Albrecht, R.A. Battye and J. Robinson, Phys. Rev. Lett. **79** (1997), 4736.
  - [4] A. Vilenkin, and A.E. Everett Phys. Rev. Lett. **48** (1982), 1867. T. Vachaspati, A.E. Everett and A. Vilenkin, Phys. Rev. **D30** (1984), 2046.
  - [5] J. Ipser and P. Sikivie, Phys. Rev. **D30** (1984), 712.
  - [6] L. Randall and R. Sundrum, Phys. Rev. Lett. **83** (1999), 4690.

- [7] H. Kodama, H. Ishihara and Y. Fujiwara, Phys. Rev. **D50** (1994), 7292. A. Ishibashi and H. Ishihara, Phys. Rev. **D56** (1997), 3446.
- [8] K. Nakamura, A. Ishibashi and H. Ishihara, Phys. Rev. D **62**, 101502R, (2000). K. Nakamura and H. Ishihara, *ibid.*, **63**, 127501, (2001).
- [9] W. Israel, Nuovo Cimento **B44** (1966), 1.
- [10] We denote  $[A] := A_+ - A_-$  for arbitrary functions  $A_{\pm}$  on  $\Sigma_{\pm}$ , respectively.
- [11] D. Kramer, H. Stephani, M.A.H. MacCallum and E. Herlt, *Exact Solutions of Einstein's Field Equations* (Cambridge: Cambridge University Press, 1980).
- [12] K. Tomita, Phys. Lett. **162B**, (1985), 287.
- [13] For a special case  $\gamma_{0\pm} = 0$  the solution is obtained in Ref. [5]
- [14] The case  $(\epsilon_-, \epsilon_+) = (-, -)$  are equivalent to  $(\epsilon_-, \epsilon_+) = (+, +)$ .
- [15] K.S. Thorne, Phys. Rev. **138**, (1965), B251.
- [16] F. Bonjour, C. Charmousis and R. Gregory, Phys. Rev. D **62**, 083504, (2000)